

Generalized Flory Theory for Rotational Symmetry Breaking of Complex Macromolecules

Josh Kelly¹, Alexander Y. Grosberg², and Robijn Bruinsma^{1,3}

¹*Department of Physics and Astronomy, University of California, Los Angeles, CA 90095, USA*

²*Department of Physics and Center for Soft Matter Research,
New York University, 726 Broadway, New York, NY 10003 and*

³*Department of Chemistry and Biochemistry, University of California, Los Angeles, CA 90095, USA*

We report on spontaneous rotational symmetry breaking in a minimal model of complex macromolecules with branches and cycles. The transition takes place as the strength of the self-repulsion is increased. At the transition point, the density distribution transforms from isotropic to anisotropic. We analyze this transition using a variational mean-field theory that combines the Gibbs-Bogolyubov-Feynman inequality with the concept of the *Laplacian matrix*. The density distribution of the broken symmetry state is shown to be determined by the eigenvalues and eigenvectors of this Laplacian matrix. Physically, this reflects the increasing role of the underlying topological structure in determining the density of the macromolecule when repulsive interactions generate internal *tension*. Eventually, the variational free energy landscape develops a complex structure with multiple competing minima.

It is well known that when attractive interactions between the units (“monomers”) of a flexible macromolecule become sufficiently strong, the molecule can undergo a folding transition from a disordered isotropic state to an ordered structure with a specific shape [1]. Less familiar is the fact that when repulsive interactions dominate, macromolecules with more complex topologies also can adopt distinct shapes. Examples are dendrimers [2] and certain biopolymers [3–6]. Their shape is determined by competing effects. On the one hand, the combination of thermal fluctuations and short-range repulsive interactions between the monomers favors isotropic swelling, since that maximizes the entropy of the molecule. If, however, the topology of the macromolecule constrains the swelling then this generates internal *tension* along the bonds and this reduces the dominance of thermal fluctuations and entropy. Swollen polymer gels [7] and polymer brushes in good solvent [8] are familiar examples of polymeric systems where swelling induces a tension that both suppresses fluctuations and confers distinct shape. The suppression of thermal fluctuations means that tense macromolecules of this type can be described by mean-field theory [8], as opposed to linear polymers that have no internal tension [7].

Suppose one gradually increases the strength of the repulsions in a soluble macromolecule with a complex topology, is there a well-defined threshold where the molecule develops a distinct shape? If there is such a threshold then what is the nature of the rotational symmetry-breaking transition and how is the resulting shape related to the underlying topology? Finally, if the number of topological constraints is increased, does a complex macromolecule eventually become over-constrained and “frustrated” with a free energy landscape that has multiple competing minima¹?

In this paper we propose a theory for the development of shape of topologically complex macromolecules for a minimal model that was introduced by Edwards to describe linear polymers and polymer gels [12, 13] in good solvent (i.e.,

solutions where repulsive interactions dominate). We construct a generalization of Flory mean-field theory and apply this to the Edwards Hamiltonian. We find that the density distribution of complex branched polymers indeed undergoes a transition where it loses rotational symmetry. The structure of the broken symmetry state is determined by the eigenvalues and eigenvectors of the *Laplacian matrix* of the molecule, a concept borrowed from graph theory. As the strength of the repulsive interactions further increases, a complex energy landscape emerges with multiple competing minima. We find that at least the coarse-grained features of the density distribution of complex macromolecules and the tension profile can be predicted on the basis of the eigenvalues and eigenvectors of the Laplacian matrix.

The Edwards Hamiltonian for a macromolecule is defined by

$$\beta H = \frac{d}{2a^2} \sum'_{i < j} (\mathbf{r}_i - \mathbf{r}_j)^2 + \sum_{i < j} u(|\mathbf{r}_i - \mathbf{r}_j|) \quad (1)$$

The summations are here over N point-like monomers located at sites \mathbf{r}_i with $i = 1, 2, \dots, N$ that are linked into a connected network by harmonic springs. The prime in H_0 , the first term on the right-hand side, indicates that this double sum is to be restricted to monomers pairs that are linked by springs. The second term in Eq.1 represents short-range repulsive monomer-monomer interactions with strength $v = \int u(r) d^d r$ and range σ in units of a . The summation now is over all monomer pairs. The Edwards Hamiltonian is realized by a network of cross-linkers connected by ideal polymer chains that have an RMS radius of gyration a .

Assume that the radius of gyration R_0 of the molecule for $v = 0$ has been determined (we will shortly see how). The radius of gyration for $v \neq 0$ can then be obtained by minimizing the Flory variational free energy [7]

$$\beta F_F(R) = \left(\frac{R^2}{R_0^2} \right) + v \frac{N^2}{R^d} \quad (2)$$

(dropping numerical coefficients). The first term on the right hand side represents entropic elasticity resisting the swelling

¹ We focus here on macromolecules with specific, prescribed structures, which is the case of interest for biomolecules. For a discussion of quenched or annealed averages over a class of structures, see refs. [9–11]

while the second term represents osmotic swelling pressure due to monomer-monomer repulsion, as expressed in second virial form. Minimizing $F_F(R)$ with respect to R^2 leads to the familiar result that $(R/R_0)^2$ increases as $(vN^2/R_0^3)^{2/5}$ in $d = 3$ when the strength of the repulsion increases. Flory theory implicitly assumes a uniform and isotropic density.

In order to allow for an anisotropic density, we first recast the Flory variational energy as a special case of the Gibbs-Bogolyubov-Feynman (GBF) variational principle [14, Section 1], which states that

$$F \leq F_T + \langle (H - H_T) \rangle_T \quad (3)$$

Here, $\langle \dots \rangle_T$ indicates that a Boltzmann average is to be taken with respect to the trial Hamiltonian H_T . F_T is the free energy associated with H_T . The variational free energy $F_V = F_T + \langle (H - H_T) \rangle_T$ provides an upper bound for the free energy.

For H_T , we will use generalized versions of H_0 expressed in terms of the eigenvectors and eigenvalues of the $N \times N$ real, square, symmetric Laplacian matrix $L_{i,j}$. The Laplacian matrix is the Laplace operator in matrix form defined on a graph of the nodes and bonds of the molecule. It has been extensively studied in the context of graph theory [15]. Diagonal entries $L_{n,n}$ are equal to the number of monomers linked to monomer n (“vertex degree”) while off-diagonal entries $L_{n,m}$ are equal to -1 if monomer n and m are linked and 0 if they are not. The rows and columns of $L_{i,j}$ add to zero so the N component vector with entries equal to one is an eigenvector with eigenvalue 0 . The other eigenvalues $\lambda^{(j)}$, with $j = 1, 2, \dots, N-1$, are strictly positive for a connected graph. The lowest non-zero eigenvalue $\lambda^{(1)}$, henceforth denoted by λ , is known as the “spectral gap”². Note that the eigenvalues and eigenvectors of the Laplacian matrix reflect only the topology of the graph of the molecule and do not relate to the geometrical space in which the molecule is embedded.

In terms of the Laplacian matrix H_0 can be written by unrestricted summation over all particles in the form $\beta H_0 = \left(\frac{d}{2a^2}\right) \sum_{i,j} L_{i,j} \mathbf{r}_i \cdot \mathbf{r}_j$. This can be usefully expressed in the

form $\beta H_0 = \frac{d}{2} \sum_{j=1}^{N-1} \lambda^{(j)} |\mathbf{A}^{(j)}|^2$ where the $\lambda^{(j)}$ are the (rank-ordered) eigenvalues of the Laplacian matrix and where the $\mathbf{A}^{(j)} = \sum_{i=1}^{N-1} \mathbf{r}_i \xi_i^{(j)} / a$ are the normal mode amplitudes. The latter are vectors in the d -dimensional embedding space but expressed in terms of the orthonormal N -component eigenvectors $\xi_j^{(j)}$ of the Laplacian matrix [19]. The mode amplitudes can be viewed as analogs of the Fourier amplitudes describing the displacements of the nodes of a graph embedded in a d -dimensional space³.

The mean square radius of gyration R_0^2 of the ideal molecule can be expressed in terms of the eigenvalues as $\frac{a^2}{N} \sum_{j=1}^{N-1} \frac{1}{\lambda^{(j)}}$ [19], which can be viewed as a generalization of the Kramers Theorem [20]. If the spectral gap λ is small compared to the higher eigenvalues then this reduces to $\lambda \simeq a^2 / (NR_0^2)$.⁴ An important unphysical feature of H_0 is that it has d zero modes (associated with translation symmetry) whereas the correct number of zero modes of a physical molecule – including translation and rotation symmetry – is $d(d+1)/2$ (3 in $d = 2$ and 6 in $d = 3$).

As a first example of the use of the variational method to include monomer-monomer interaction, assume that H_T equals H_0 except that the lowest non-zero eigenvalue, the spectral gap λ , is replaced by a variational parameter γ . So:

$$\beta H_T = \frac{d}{2} \gamma |\mathbf{A}^{(1)}|^2 + \frac{d}{2} \sum_{i=2}^{N-1} \lambda^{(i)} |\mathbf{A}^{(i)}|^2 \quad (4)$$

This leads to a variational free energy:

$$\beta F_V(\gamma) \simeq \frac{d}{2} \left(\ln \gamma + \frac{\lambda}{\gamma} \right) + C(N) \frac{v}{a^d} \left(\frac{\gamma d}{2\pi} \right)^{d/2} \quad (5)$$

where $C(N) = \sum_{m < n=1}^N ((\xi_m - \xi_n)^2 + \gamma \sigma^2)^{-d/2}$ with ξ_m the eigenvector associated with the spectral gap λ and σ the range of the excluded volume interaction in units of a (the derivation is given in [14, Section III]). Using the normalization $\sum_{m=1}^N \xi_m^2 = 1$ and assuming a (large) random structure gives $C(N) \propto N^{2+d/2}$. The resulting variational expression reduces to Flory mean-field theory if one replaces γ by $a^2 / (NR^2)$.

Next, allow for the possibility of an anisotropic density by including in H_T non-zero expectation values $\mathbf{A}_0^{(i)}$ for the M mode amplitudes with the lowest M eigenvalues:

$$\beta H_T = \frac{d}{2} \left(\sum_{i=1}^M \gamma^{(i)} \left(\mathbf{A}^{(i)} - \mathbf{A}_0^{(i)} \right)^2 + \sum_{i=M+1}^N \lambda^{(i)} |\mathbf{A}^{(i)}|^2 \right) \quad (6)$$

The special case $\gamma^{(i)} = \lambda^{(i)}$ and $M = N$ is interesting. The set of order-parameters $\mathbf{A}_0^{(i)}$ then defines a set of N particle vectors $\mathbf{r}_{0j}/a = \sum_{i=1}^{N-1} \mathbf{A}_0^{(i)} \xi_j^{(i)}$ (up to an overall translation). Expressing the trial Hamiltonian in real space leads to:

$$\beta H_T = \frac{d}{2a^2} \sum'_{i < j} (\mathbf{r}_i - \mathbf{r}_j - \Delta \mathbf{r}_{0ij})^2 \quad (7)$$

where $\Delta \mathbf{r}_{0ij} = (\mathbf{r}_{0i} - \mathbf{r}_{0j})$. This is similar to the Hamiltonian of the ideal molecule except that Gaussian bonds $\mathbf{r}_i - \mathbf{r}_j$ linking monomers i and j have been placed under internal tension so the expectation value of the bond separation $\Delta \mathbf{r}_{0ij}^0$ has a

² Analytical expressions for the eigenvalues are available for linear chains, cubic lattices, dendrimers, and a variety of fractal structures [16–18]. Efficient algorithms are available for the numerical computation of the eigenvalues and eigenvectors.

³ Examples of eigenvalues and eigenvectors of the Laplacian matrix and of the normal modes are given in [14, Section II]

⁴ For the case of the ring polymer in [14, Section II], the computation of the mean square radius of gyration reproduces the standard result that $R_0^2 \propto N$. The $\mathbf{A}^{(1)}$ spectral gap mode corresponds to an expansion of the N particles from a point to a ring with radius $|\mathbf{A}^{(1)}|$.

certain direction in space. Formally, Eq.7 is identical to the Gaussian Network Model that is frequently used to obtain the normal modes of folded proteins [21]. It also has the appropriate number of zero modes.

Next, include both types of variation. The simplest case is again $M = 1$:

$$\beta F_V(\gamma, \mathbf{A}_0) \simeq \frac{d}{2} \ln \gamma + \frac{d}{2} \lambda \left(|\mathbf{A}_0|^2 + \frac{1}{\gamma} \right) + C(N) \frac{v}{a^d} \left(\frac{\gamma d}{2\pi} \right)^{d/2} e^{-\gamma d \mathbf{A}_0^2/2} \quad (8)$$

The function $F_V(\gamma, |\mathbf{A}_0|)$ always has a stable minimum at $|\mathbf{A}_0| = 0$, which corresponds to Flory theory, but the surface $F_V(\gamma, \mathbf{A}_0)$ has a second minimum for a large γ and a non-zero value of $|\mathbf{A}_0|$. The density distribution described by this minimum has a stretched, linear shape with particle locations determined by the eigenvector ξ_m of the Laplacian matrix associated with the spectral gap. As a function of increasing v/a^d , the absolute minimum usually shifts discontinuously from the Flory minimum to the new minimum. An exception is the case of a linear chain when the Flory minimum is the absolute minimum for any v .

While the $M = 1$ theory is analytically tractable, it can be shown that it only allows for linearly stretched shapes and that it is necessary to include multiple modes to completely lift the overlap between particles [14, Section I]. The variational free energy $F_V(\{\gamma^{(i)}, \mathbf{A}_0^{(i)}\})$ for M coupled vectorial order parameters is a natural extension of Eq. 8 (derived in [14, Section III]) but minimization of $F_V(\{\gamma^i, \mathbf{A}_0^{(i)}\})$ requires numerical methods. Numerical minimization of $F_V(\{\gamma^i, \mathbf{A}_0^{(i)}\})$ for a second-generation dendrimer in $d = 2$ showed that for increasing v/a^d , there is now a whole series of transitions where modes with increasing eigenvalues “freeze out”. Importantly, the interacting system has the correct number of zero modes in $d = 2$. The numerical minimization of $F_V(\{\gamma^i, \mathbf{A}_0^{(i)}\})$ for a 36-node branched graph with a maximum of $M = 18$ mode expectation values is shown in Fig. 1. For v/a^2 less than about 0.75, the isotropic Flory minimum was the lowest free energy state, as illustrated by the case $v/a^2 = 0.24$. However, for $v/a^2 = 1.20$ the density profile is quite anisotropic with three diffuse maxima. The power spectrum of mode amplitudes in this state is dominated by the lowest few eigenvalues. For $v/a^2 = 2.05$, all of the $M = 18$ modes have gained non-zero expectation values and the power spectrum is more complex with a second peak at larger eigenvalues. Note that the density profile is quite detailed. The system appears to be frozen. However, the numerical minimization of the variational free energy was, for larger values of v/a^2 , significantly complicated by the fact that the variational free energy clearly had numerous minima with comparable energies. The last density profile should be viewed only as representative.

For comparison, we also performed a $d = 2$ Monte-Carlo (MC) simulations on the same system (Fig.2). One of the nodes was pinned to suppress rigid-body Brownian motion of the center of mass. The Kabsch algorithm [22] was used to compensate for rigid-body rotational Brownian motion. The

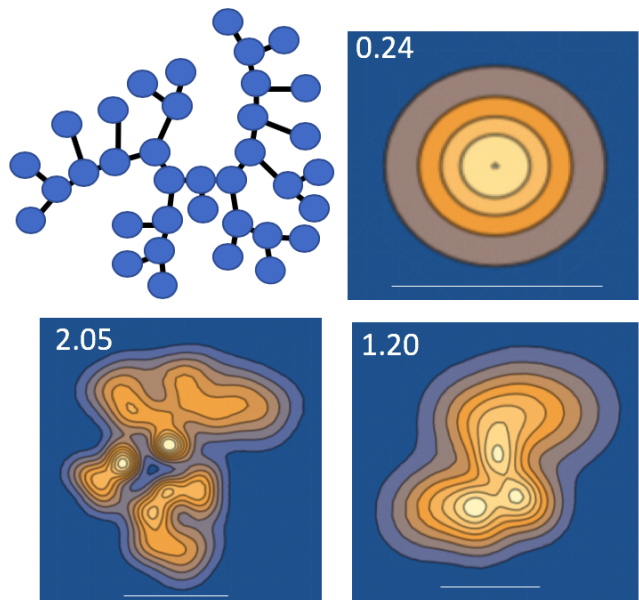


FIG. 1. Two-dimensional density profiles obtained using the GBF variational method for a 36 node branched polymer with a maximum of $M = 18$ non-zero mode expectation values. Top left: Graph of the molecule. Top right: $v/a^2 = 0.24$ in units of $k_B T$. The density profile is isotropic. Bottom right: $v/a^2 = 1.20$. A few low-lying modes have condensed. Bottom left: $v/a^2 = 2.05$. Most modes have condensed. White space bar: $5a$

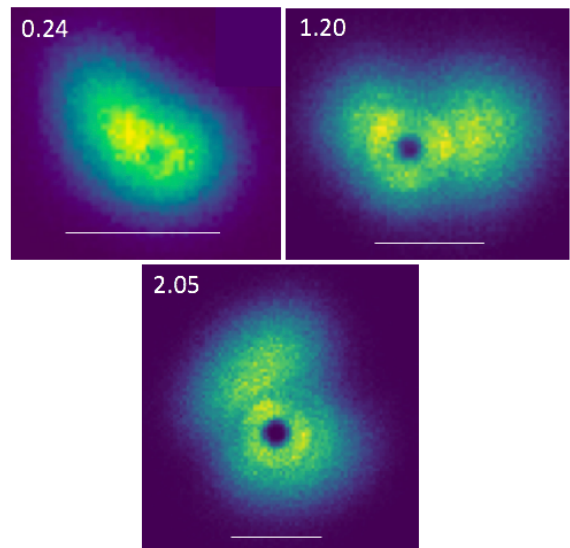


FIG. 2. Density profiles obtained by Monte-Carlo simulation for the same molecule and interaction strengths as Fig. 1. White space bar: $5a$.

top left image in Fig.2, with $v/a^2 = 0.24$, has a radius of gyration comparable to the theoretical prediction and a weak but noticeable rotational asymmetry. For $v/a^2 = 1.20$, the predicted and computed densities have comparable sizes and both have three maxima. The onset of rotational asymmetry thus appears to be less sharp than predicted by the theory while for $v/a^2 = 2.05$ the theoretical density profile is significantly more detailed than the computed profile. The MC simulations were, in this last case, complicated by long relaxation times.

As an alternative route for a quantitative test of the theory, we compared the moduli $|\Delta\mathbf{r}_{0i,j}|$ of the bond extensions predicted by the GBF variational principle with those obtained from the MC simulation. We found that the variational method correctly obtains the bond extensions of the outer monomers while it somewhat overestimates the bond extensions of the inner monomers ([14, Section IV]). Note that the development of significant internal tension provides an *a-posteriori* justification of the use of a self-consistent mean-field theory. The agreement in terms of the bond tensions but not in terms of detailed density profiles indicates that the competing free energy minima may have similar patterns of bond tension. An important extension of the theory would be to allow for the fact that this is a finite system with multiple minima computing to the free energy. This would lead to “smearing” of the rotational symmetry breaking transition.

A natural area where this theory can be applied is that of biopolymers with non-trivial topology that are dominated by repulsive interactions. An increasing number of functional but disordered proteins has been identified. The interactions between the different parts of these proteins are predominantly repulsive (“good solvent”) yet they have distinct, reproducible shapes [3, 4], as confirmed by Molecular Dynamics simulations [5]. Though proteins have a linear polymer primary structure, they still can effectively adopt a complex topology due to attractive interactions between specific residues, for instance between cysteine residues that can form disulfide bridges. Another possible area of application involves the

shape of large, single-stranded RNA molecules. A graph of the secondary structure of an RNA molecule has a branched topology without circuits, The tertiary structure of an RNA molecule is generated by pairing between non-adjacent nucleic acids that were not paired as part of the secondary structure and these tertiary contacts could be included as bonds in the graph of the molecule, which would produce cycles. Cryo-EM studies of large, swollen single-stranded RNA molecules in good solvents reveal that they are disordered but their density profile has a distinct anisotropy [23]. Current methods of DNA origami allow for the construction of molecular structures with prescribed topologies that are reasonably represented by the Edwards Hamiltonian, which allows for direct experimental tests of the proposed theory. A rotational symmetry breaking transition could be engineered by changing the solvent quality. We close by noting that there is a related problem where the method discussed in this paper could be applied namely the computation of the most likely structure of a biopolymer for which it already has been experimentally determined that certain elements of the primary structure are adjacent to each other, for example in the form of a contact map obtained by NMR [24]. Though the distance constraints are here *knowledge-based*, instead of physical bonds or links, the Laplacian matrix method still could be used to encode the NMR contact map after which likely density profiles could be computed using the method we outlined here.

ACKNOWLEDGMENTS

RB thanks Alex Levine for useful discussion and acknowledges support from NSF-DMR under Grant 1006128 and from the Simons Foundation. Both A.Y.G. and R.B. wish to acknowledge the Aspen Center for Physics supported by the National Science Foundation (USA) under Grant No. PHY-1066293 where this work was started.

-
- [1] Vijay S Pande, Alexander Yu Grosberg, and Toyochi Tanaka. Heteropolymer freezing and design: towards physical models of protein folding. *Reviews of Modern Physics*, 72(1):259, 2000.
 - [2] David Boris and Michael Rubinstein. A self-consistent mean field model of a starburst dendrimer: Dense core vs dense shell. *Macromolecules*, 29(22):7251–7260, 1996.
 - [3] Feng Ding, Ramesh K Jha, and Nikolay V Dokholyan. Scaling behavior and structure of denatured proteins. *Structure*, 13(7):1047–1054, 2005.
 - [4] Peter Zipper and Helmut Durchschlag. Modelling of bacteriophage capsids and free nucleic acids. *Applied Crystallography*, 40(s1):s153–s158, 2007.
 - [5] Vytautas Gapsys and Bert L de Groot. Optimal superpositioning of flexible molecule ensembles. *Biophysical journal*, 104(1):196–207, 2013.
 - [6] Ajaykumar Gopal, Z.H. Zhou, Charles M. Knobler, and William M. Gelbart. Visualizing large RNA molecules in solution. *RNA*, 18:284–299, 2012.
 - [7] Alexander Y. Grosberg and Alexei R. Khokhlov. *Statistical Physics of Macromolecules*. American Institute of Physics Press, 1994.
 - [8] Scott T Milner, TA Witten, and ME Cates. Theory of the grafted polymer brush. *Macromolecules*, 21(8):2610–2619, 1988.
 - [9] A. Grosberg and S. Nechaev. From statistics of regular tree-like graphs to distribution function and gyration radius of branched polymers. *J. Phys. A: Math. Theor.*, 48:345003, 2015.
 - [10] Yacov Kantor and Mehran Kardar. Collapse of randomly linked polymers. *Physical review letters*, 77(20):4275, 1996.
 - [11] Alexander Grosberg, Alexander Gutin, and Eugene Shakhnovich. Conformational entropy of a branched polymer. *Macromolecules*, 28(10):3718–3727, 1995.
 - [12] RC Ball and SF Edwards. Elasticity and stability of a dense gel. *Macromolecules*, 13(3):748–761, 1980.
 - [13] RT Deam and SF Edwards. The theory of rubber elasticity. *Philos. Trans. R. Soc., London*, A 280:317, 1976.

- [14] See supplemental material at [URL will be inserted by publisher].
- [15] Leonid E. Zhukov. Diffusion and random walks on graphs (lecture notes), March 2015.
- [16] Hongxiao Liu and Zhongzhi Zhang. Laplacian spectra of recursive treelike small-world polymer networks: Analytical solutions and applications. *The Journal of Chemical Physics*, 138(11):114904, 2013.
- [17] Maxim Dolgushev, Hongxiao Liu, and Zhongzhi Zhang. Extended Vicsek fractals: Laplacian spectra and their applications. *Physical Review E*, 94(5):052501, 2016.
- [18] Alafate Julaiti, Bin Wu, and Zhongzhi Zhang. Eigenvalues of normalized Laplacian matrices of fractal trees and dendrimers: Analytical results and applications. *The Journal of Chemical Physics*, 138(20):204116, 2013.
- [19] Kohhei Nitta. A topological approach to statistics and dynamics of chain molecules. *The Journal of Chemical Physics*, 101(5):4222–4228, 1994.
- [20] Michael Rubinstein and Ralph H. Colby. *Polymer Physics*. OUP Oxford, 2003.
- [21] Turkan Haliloglu, Ivet Bahar, and Burak Erman. Gaussian dynamics of folded proteins. *Physical review letters*, 79(16):3090, 1997.
- [22] Wolfgang Kabsch. A solution for the best rotation to relate two sets of vectors. *Acta Crystallographica Section A: Crystal Physics, Diffraction, Theoretical and General Crystallography*, 32(5):922–923, 1976.
- [23] Ajaykumar Gopal, Z Hong Zhou, Charles M Knobler, and William M Gelbart. Visualizing large RNA molecules in solution. *RNA*, 2011.
- [24] AM Gutin and EI Shakhnovich. Statistical mechanics of polymers with distance constraints. *The Journal of chemical physics*, 100(7):5290–5293, 1994.